

RESEARCH REPORT

Xq26.3 Microdeletion in a Male with Wildervanck Syndrome

Khaled K. Abu-Amero^{1,4}, Altaf A. Kondkar¹, Ibrahim A. Alorainy², Arif O. Khan³,
Leila A. Al-Enazy⁴, Darren T. Oystreck^{1,5}, and Thomas M. Bosley¹

¹Department of Ophthalmology, College of Medicine, King Saud University, Riyadh, Saudi Arabia, ²Radiology Department, College of Medicine, King Saud University, Riyadh, Saudi Arabia, ³The King Khaled Eye Specialist Hospital, Riyadh, Saudi Arabia, ⁴Department of Ophthalmology, College of Medicine, University of Florida, Jacksonville, FL, USA, and ⁵Division of Ophthalmology, Faculty of Health Sciences, University of Stellenbosch, Tygerberg, South Africa

ABSTRACT

Background: Wildervanck Syndrome (WS; cervico-oculo-acoustic syndrome) consists of Duane retraction syndrome (DRS), the Klippel-Feil anomaly, and congenital deafness. It is much more common in females than males and could be due to an X-linked mutation that is lethal to hemizygous males. We present the genetic evaluation of a male with WS and his family.

Materials and Methods: Clinical evaluation and neuroimaging, sequencing of candidate genes, and array comparative genomic hybridization.

Results: The patient had bilateral type 1 DRS, fusion of almost the entire cervical spine, and bilateral severe sensorineural hearing loss due to bilateral cochlear dysplasia; he also had congenital heart disease requiring surgery. His parents were unrelated, and he had eight unaffected siblings. The patient had no mutation found by Sanger sequencing of *HOXA1*, *KIF21A*, *SALLA*, and *CHN1*. He had a 3kB deletion in the X-chromosome at Xq26.3 that was not found in his mother, one unaffected sibling, or 56 healthy controls of matching ethnicity. This deletion encompassed only one gene, Fibroblast Growth Factor Homologous Factor 13 (*FGF13*), which encodes a 216-amino acid protein that acts intracellularly in neurons throughout brain development.

Conclusions: Analysis of this patient's phenotype and genotype open the possibility that X-chromosome deletions may be a cause of WS with larger deletions being lethal to males and that *FGF13* mutations may be a cause of WS.

Keywords: Cervico-oculo-acoustic syndrome, chromosome deletion, congenital deafness, Duane retraction syndrome, Klippel-Feil anomaly, Wildervanck syndrome, x-linked

INTRODUCTION

Wildervanck syndrome (WS, OMIM 314600), or the cervico-oculo-acoustic syndrome,¹ is an uncommon^{1,2} congenital syndrome defined by the co-occurrence of the Klippel-Feil anomaly (congenital fusion of cervical vertebra; OMIM 118100), Duane retraction syndrome (DRS, OMIM 126800), and congenital deafness that may be sensorineural, conductive, or mixed.³ There have been reports of WS patients with additional

features such as cervical spinal cord developmental abnormalities,^{4,5} facial palsy,⁶ other neurologic developmental abnormalities,⁷ cardiac abnormalities,⁸ cleft palate,^{2,9} and ectopia lentis. The possible genetic etiology of the syndrome is not yet defined, but the fact that it occurs much more commonly in females¹ has led to the hypothesis that it is an X-linked disorder that is lethal to hemizygous males.¹⁰

We describe the phenotype of a male with sporadic WS, including congenital heart disease requiring

Received 23 October 2012; revised 4 December 2012; accepted 9 January 2013; published online 1 February 2013

Correspondence: Khaled K. Abu-Amero, PhD, FRCPath, Department of Ophthalmology, College of Medicine, King Saud University, Riyadh, Saudi Arabia. Tel: +96646781000. Fax: +96614775724. Email: abuamero@gmail.com

surgery in early childhood, who had a microdeletion in the X-chromosome.

MATERIALS AND METHODS

Patient Information

The patient was examined and his chart reviewed. The proband's father was deceased and his mother signed informed consent approved by the IRB at College of Medicine of King Saud University, Riyadh, Saudi Arabia.

Sample Collection and DNA preparation

Blood samples (5 ml) were drawn in EDTA (ethylenediaminetetraacetic acid) tubes. Tubes were centrifuged at 5500g for 5 min and the buffy layer was used for DNA extraction using the illustra blood genomicPrep Mini Spin Kit (GE Healthcare, Buckinghamshire, UK) and stored at -20°C in aliquots until further use.

Sequencing of Genes Associated with Syndromic DRS (HOXA1, KIF21A, SALL4 and CHN1)

The full coding region of the *Homo sapiens* homeobox A1 (*HOXA1*) gene, exon-intron boundaries, and promoter region were sequenced utilizing primers and PCR conditions described previously.¹¹ The full coding regions of the sal-like 4 (*SALL4*) and chimerin 1 (*CHN1*) genes were sequenced according to protocols described previously.^{12,13} Exons 8, 20, and 21 of the kinesin family member 21A (*KIF21A*) gene were sequenced as those exons are considered hotspots for mutations in this gene.¹⁴

Array Comparative Genomic Hybridization (Array CGH)

The Affymetrix Cytogenetics Whole-Genome 2.7M array (Affymetrix Inc., Santa Clara, CA, USA) was used to detect known and novel chromosomal aberrations across the entire genome. The array provides high density coverage of over 400,000 SNP markers and 2.3 million non-polymorphic markers with high density coverage across cytogenetically significant regions; it covers all annotated genes, cancer genes, X-chromosome genes, cytogenetics relevant or haploinsufficiency genes to allow the detection of loss of heterozygosity, uniparental disomy, and regions identical-by-descent. The array provides a superior resolution for detection of smaller structural

variations with a median distance between markers of 735bp and of 294bp within cancer gene loci. The assay was performed according to the manufacturer's instructions using the reagents provided with the kit. Briefly, for each investigated sample, 150ng of high quality genomic DNA was subjected to denaturation and neutralization steps followed by whole-genome amplification reaction at 30°C for 16h. After amplification, purification was performed using magnetic beads on a Costar round bottom plate (Corning Inc., Corning, NY, USA) and magnetic-ring stand (Applied Biosystems, Foster City, CA, USA). Purified DNA was then quantified using NanoDrop 2000c (Thermo Scientific, Wilmington, DE, USA) with an average yield of amplified DNA of $>1\ \mu\text{g}/\mu\text{l}$. Purified DNA was then subjected to simultaneous fragmentation and labeling reaction at 37°C for 2h, following which the sample was denatured and loaded into a single array for hybridization. Hybridization was performed in a GeneChip[®] Hybridization Oven 645 (Affymetrix) for 16–19h at 50°C , rotation of 60rpm. After hybridization, the chip was washed and stained using the GeneChip[®] Fluidics Station 450 (Affymetrix) and scanned using the GeneChip[®] Scanner 3000 7G (Affymetrix).

Analysis of Array CGH Data

Data were analyzed using the Affymetrix[®] Chromosome Analysis Suite v1.2 (ChAS) software (Affymetrix Inc. CA, USA). In the absence of internationally recognized criteria for analysis of high resolution array CGH results, we devised new, preliminary criteria to ensure accuracy of, and to avoid analysis of, copy number variations that are probably not pathologic. Therefore, a copy number variation had to satisfy all the following conditions to be considered potentially pathologic: (1) it was not reported in the Database of Genomic Variants (DGV; <http://projects.tcag.ca/variation/>) among normal controls; (2) it was not present in at least 50 healthy controls of similar ethnicity; (3) it segregated with the phenotype and was not present in unaffected family members; and (4) it included an area of the genome encompassing one or more functional genes. The threshold for gain or loss was adjusted to 10kb. We used the National Center for Biotechnology Information human genome assembly Build 35.

Quantitative PCR for Deletion Confirmation

A semi-quantitative PCR method was used to confirm the array CGH findings by measuring the intensity of the gene encompassed by the detected chromosomal variation. Labeled primers were designed to encompass part of exon 2 of the *FGF13* gene. FAM labeled

forward primer 6-FAM GGT GTG GGT GTA GGG AGA GA and unlabeled reverse primer GCT TGG TCA CCT TTC CAC TC were used to amplify a fragment of 220bp in size. The detailed PCR protocol was described previously.¹⁵ Briefly, Polymerase chain reactions were performed using 100ng of DNA, 5 pmoles of each oligonucleotide primer, 200 μ M of each dNTP, 1 unit of HotStar Taq-polymerase (Qiagen, Valencia, CA) and 1X PCR buffer in a 20 μ l volume. The PCR program started with a 95 °C denaturation for 5 min, followed by 25 cycles of 95 °C for 1 min, 57 °C for 45 sec, and 72 °C for 1 min. PCR samples were electrophoresed on the 3130xl Genetic Analyzer (Applied Biosystems, Foster City, CA), and sizes and fluorescence peak intensities were recorded.

RESULTS

Patient Evaluation

The proband was the product of a normal pregnancy and delivery but was deaf from birth with an unusually short neck. His parents were unaffected with Klippel-Feil anomaly, deafness, or DRS. They were not related, his father was dead, and he had eight unaffected siblings (Figure 1A). He had no other dysmorphism, but his parents also noticed an ocular motility abnormality shortly after birth. He had a ventricular septal defect and an atrial septal defect requiring surgery at age 2.5 years, and post-operatively he had a right phrenic nerve palsy, transient pulmonary hypertension, and recurrent chest infections. He had profound sensorineural hearing loss with delayed speech development.

Cognitive function seemed normal, and his mother denied any other major general medical problems.

On neuro ophthalmologic examination at age 12 years, the patient was a bright, cooperative, deaf, mute young man. Afferent visual functioning was normal bilaterally with normal globes, ocular fundi, and visual acuity. He had bilateral type 1 DRS with retraction of the globes and narrowing of the palpebral fissures OU on adduction (Figure 2). He had a substantial up shoot of the left eye on right gaze, and a down shoot of the right eye on left gaze, but vertical gaze was otherwise normal. In primary gaze he had an esotropia with a mild left hypertropia. He was completely deaf bilaterally and mute, although very responsive to his surroundings. Cognitive function was grossly normal, and the remainder of his neurologic exam was unremarkable. He had a short neck with a low hair line, reduced neck mobility, and shoulders held in an elevated position.

A CT scan of the neck confirmed complete fusion of the vertebral bodies of C1 and C2 with a rudimentary intervertebral disc between C2 and C3 and complete fusion of C3 to C6 (Clarke¹⁶ classification KF4; Figure 3). Fusion involved the lateral masses of the cervical vertebrae from C2 through C6 and of the spinous processes from C3 to C5. The posterior arch of C1 and the spinous process of C2 were absent. A small posterior cleft was seen in the body of C2 and lower part of the clivus. The foramen magnum was wide, but no cerebellar tissue was herniating.

No supratentorial brain abnormality was identified on MRI. However, a small neuroenteric cyst was present anterior to the ponto-medullary junction slightly compressing the medulla on the left side (Figure 4), and abducens nerves were not visible on

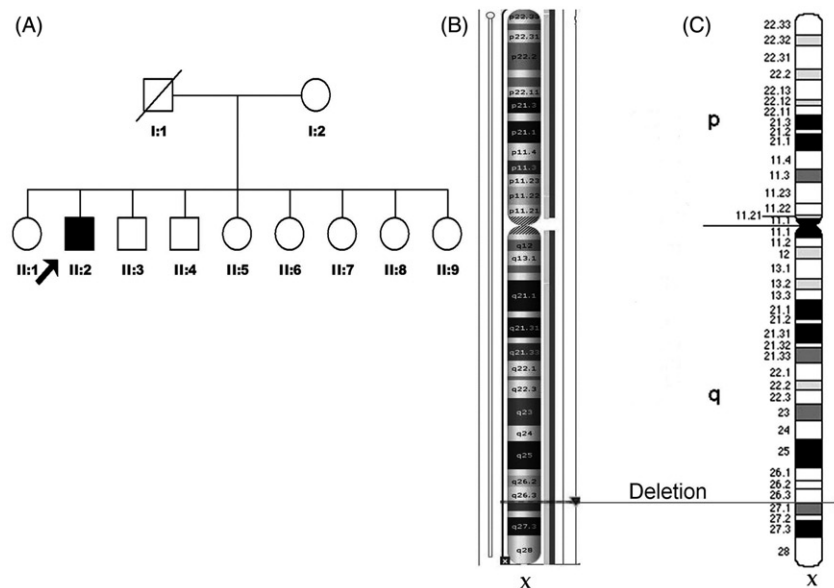


FIGURE 1. Pedigree and array CGH results. (A) Pedigree of proband's family. He has eight unaffected siblings. The results of the array CGH after analysis by ChAS showing (B) the position of the deletion on chromosome X and (C) an ideogram of chromosome X with line crossing through the cytogenetic band Xq26.3 indicating the location of the deletion.



FIGURE 2. Ocular motility. Ocular motility montage showing (A) right gaze, (B) primary gaze, and (C) left gaze. He had bilateral type 1 DRS with retraction of the globes and narrowing of the palpebral fissures OU on adduction. He had a substantial up shoot of the left eye on right gaze (A), and a down shoot of the right eye on left gaze (C), but vertical gaze was otherwise normal. In primary gaze (A) he had an esotropia with a mild left hypertropia. He had no diplopia and was easily able to fixate with either eye.

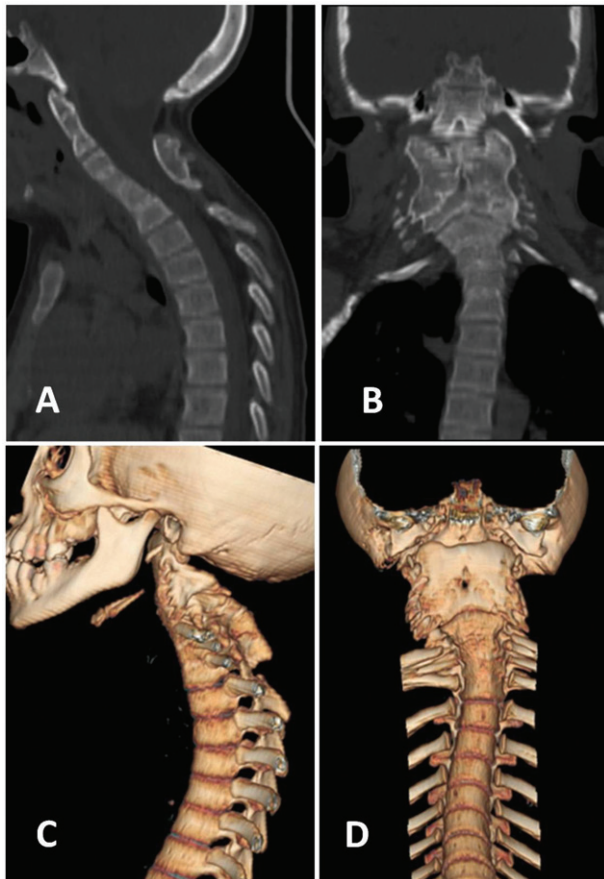


FIGURE 3. Klippel-Feil anomaly. Reformatted CT images of the cervical spine in (A) sagittal, and (B) coronal planes showing fusion of vertebral bodies, lateral masses, and spinous processes of the cervical spine with wide foramen magnum. (C) Lateral, and (D) cranially angulated frontal 3D images clearly show cervical spine fusion and short neck. The cervical spine appears like one piece of bone (B and D). Image (D) was reconstructed after removal of the facial bones to allow adequate view of the craniocervical junction.

either side. A large posterior cleft incompletely split the lower medulla and upper cervical spinal cord into two halves, constituting incomplete diastematomyelia.⁴

He had bilateral inner ear malformations (Figure 5). The cochleae were dilated and dysplastic bilaterally, more on the left, with some development of the basal turn, but the remaining turns were featureless and dilated. The vestibule and semicircular canals were

completely absent on the right side, while on the left side the vestibule was dilated and dysplastic, and the semicircular canals were absent except for a dilated, dysplastic posterior semicircular canal. The middle ear ossicles on both sides were hypoplastic. Internal auditory and facial canals were unremarkable bilaterally with cochlear nerves visible on both sides, but the left jugular bulb was high and dehiscent.

HOXA1, KIF21A, SALL4 and CHN1 Sequencing

No sequence change was detected in *HOXA1*, *SALL4* and *CHN1* after sequencing the full coding region of the genes. No sequencing changes were detected after sequencing exon 8 and 21 (hot spot area for mutations) of the *KIF21A* gene.

Array CGH Results

Array CGH documented a partial deletion of chromosome X extending from 137,779,548 to 137,782,146 (total size 3 kb) at Xq26.3 cytogenetic band (Figure 1B, 1C). The copy number state was equal to 0, indicating that this deletion is likely to be hemizygous. The confidence value calculated by the chromosomal analysis software (ChAS) was 99% with a marker count of 15 spanning the deleted area. This deletion was likely to be *de novo* and segregated with the syndrome described here because it was not detected in the proband's mother, an unaffected brother, and 56 unrelated healthy individuals of similar ethnicity. The father was deceased, but was reported to have been normal and free of the phenotype present in his son. The deleted area on chromosome X was confirmed by semi-quantitative PCR method as detailed above. The mean (\pm SD) of three separate readings of fluorescence peak intensities was 123 (\pm 39) for the proband, 54928 (\pm 87) for the unaffected brother, and 55008 (\pm 64) for a normal male control. The DGV had no reported chromosomal deletion(s) or duplication(s) in the deletion region.

The deleted 3 kb region are in the middle of only one gene which is the Fibroblast Growth Factor

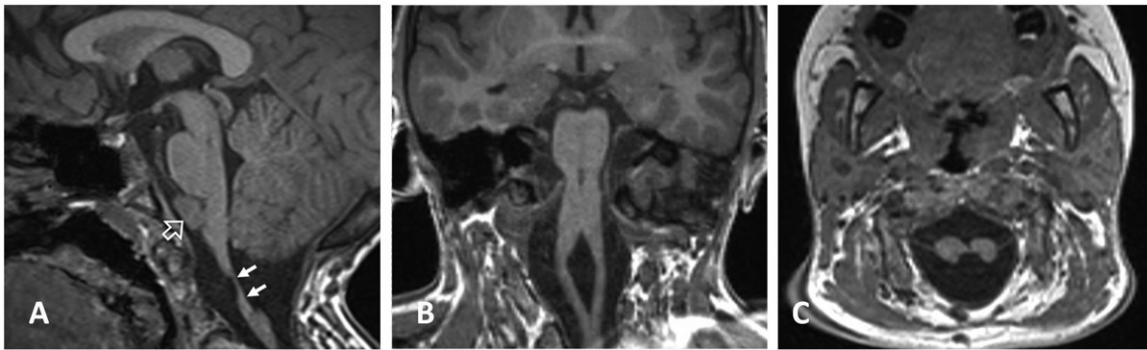


FIGURE 4. Brainstem and spinal cord. (A) Sagittal, (B) coronal, and (C) axial T1-weighted MR images of the brain showing brainstem changes in the patient. A neuroenteric cyst (open arrow on A) is located anterior to the pontomedullary junction. The lower medulla and upper cervical spinal cord have a large posterior cleft causing an incompletely split cord and appearing on mid-sagittal image as thinning of medulla (solid arrows on A). A smaller anterior cleft is apparent on sagittal (A) and axial (C) images. The foramen magnum is wide, but no cerebellar tissue is herniating.

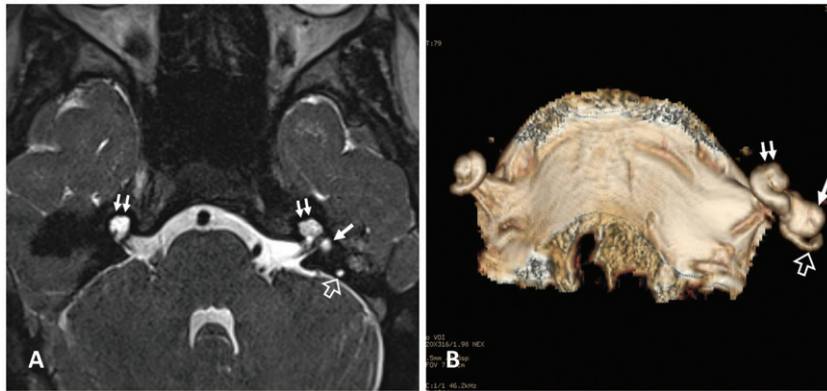


FIGURE 5. Inner ear malformation. High resolution T2-weighted MR image of (A) the temporal bone, and (B) a 3D reconstruction of the inner ear structures show bilateral cochlear dilatation and dysplasia (double arrows) with lack of normal development of cochlear turns except for partial development of the basal turn. The degree of cochlear dilatation and dysplasia is more remarkable on the left side (B). The left vestibule (solid arrow) is also dilated and dysplastic with absence of the semicircular canals except the posterior semicircular canal (open arrow) that also appears dysplastic (dilated with irregular outline). The vestibule and semicircular canals on the right side are completely absent.

Homologous Factor 13 gene (Gene Symbol: *FGF13*). This gene encodes a 216-amino acid protein with a calculated molecular mass of 22 KD. It belongs to a subclass of fibroblast growth factors that are expressed in neurons of the developing and adult central nervous system.¹⁷

DISCUSSION

We describe a male who meets the clinical criteria for WS,¹ including bilateral type 1 DRS (Figure 2), type 1 Klippel-Feil anomaly causing almost complete fusion of the cervical vertebral bodies (Figure 3), and bilateral deafness with inner ear malformations involving the cochlea, vestibules, and semicircular canals (Figure 5). Neuroimaging revealed malformations of the lower brainstem and cervical spinal cord (Figure 4) with incomplete diastematomyelia, as reported previously.⁴ However, this patient was male, which occurs infrequently in WS.^{1,18,19}

In addition, he had congenital heart disease requiring surgery during early childhood, which is also uncommon in WS.²⁰ His parents were not related, and the occurrence of WS in this patient, as in most patients,¹⁸ seemed to be sporadic.¹

Interestingly, this young man also met the major clinical criteria of Bosley-Salih-Alorainy syndrome (BSAS), with bilateral DRS, bilateral congenital deafness, and a cardiovascular developmental abnormality.^{21,22} No previous individual with BSAS has had a Klippel-Feil anomaly, but some individuals have had clubfoot and other anatomic dysmorphism.²¹ Of course, BSAS is an unlikely diagnosis because he did not have homozygous mutations identified in the *HOXA1* gene.¹¹ He also had no identified mutations in other genes reported to cause syndromic DRS, including *KIF21A*, *SALL4*, and *CHN1*.

High resolution array CGH revealed a microdeletion (3 kb) in the X-chromosome that affected only the *FGF13* gene at Xq26.3. *FGF13* and other fibroblast growth factor homologous factors (FHF) genes are

expressed by neurons throughout brain development with different neuronal types often having different FHF gene expression profiles.²³ FHF genes act intracellularly, binding to microtubules, voltage-gated sodium channels, and certain other intracellular scaffold proteins.^{24,25} They play a role in the patterning of neural primordium, proliferation of neural progenitors, neuronal migration, axon navigation, and synaptogenesis.²⁶ Northern blot analysis confirmed prominent expression of *FGF13* in human fetal and adult brain,²³ particularly in cerebellum and cortex¹⁷ with tissue-specific alternative splicing and alternative transcription starts.²⁷ *FGF13* is enriched in axonal growth cones, and the loss of *FGF13* impairs neuronal polarization and increases the branching of axons and leading processes.²⁵ Array CGH results in this patient may imply that *FGF13* can influence the development of the abducens cranial nerve, the inner ear, and the cervical spine.

The clinical characteristics of WS are quite variable in terms of cause and degree of deafness, presence and pattern of ocular motility disturbance, characteristics of the cervical spine abnormality, and potential additional presence of brainstem developmental anomalies, other vertebral and orthopedic abnormalities, and speech and neck developmental abnormalities.¹ No genetic etiology of WS has been reported previously, although the largely sporadic character and female predominance of the syndrome has led to the hypothesis that it is due to a lethal mutation on the X chromosome.^{28–30} Therefore, the occurrence of a presumably *de novo* (the father was deceased) deletion on the X chromosome in this patient seems unlikely to be a coincidence. *FGF13* is a plausible candidate for the phenotypic characteristics of this patient given that the deletion of *FGF13* in mice results in neuronal migration defects²⁵ and that a related gene (*FGFR3*) has been reported in relation to Klippel-Feil anomaly.³¹

This patient represents a unique variant of WS because he is a male with a history of symptomatic congenital heart disease; therefore, it is difficult to generalize from his phenotype and genotype. Nevertheless, high resolution array CGH has not been employed previously to investigate WS, leaving open the possibility that a deletion in the X-chromosome similar to that described here may be a common cause of WS. Survival of this patient may be due in part to the fact that his deletion was tiny and involved only one gene. If chromosome X deletions can be the cause of WS, the clinical presentation of this patient implies that deletion of the *FGF13* gene alone is capable of causing a severe WS phenotype.

Larger chromosome X deletions might affect additional genes that at times impart lethality to males. The closest genes upstream begin at a distance of 800 Kb and include: (1) *RBMX* (RNA binding motif protein with possible involvement of the

spermatogenesis); (2) *GPR101* (G protein-coupled receptor 101; a gene with unknown function); and (3) *SNORD61* (small nucleolar RNA with regulatory function). Likewise, the three closest genes downstream begin at a distance of 1900 Kb and are: (1) *MCF2* (cell line derived transforming sequence with unknown exact function); (2) *ATP11C* (probable phospholipid-transforming ATPase IG); and (3) *CXorf66* (chromosome X open reading frame 66, with no exact function known). With our current knowledge, it is impossible to reliably predict the consequences of a larger deletion encompassing these and other genes surrounding *FGF13*, since exact function of many nearby genes are not known.

This patient is an example of the association of DRS with congenital deafness. This association has been reported previously in BSAS,¹¹ thalidomide embryopathy,³² other disturbances of the HOX cascade,^{33–35} and other chromosomal syndromes.³⁶ In addition, heterozygous *SALL4* mutations are sometimes associated with DRS and congenital deafness, quite likely because *SALL4*, like *HOXA1*, is active during early brainstem development.^{37,38} It is perhaps not surprising that genetic (HOX cascade, SALL family of genes) or teratogenic disruption of genes being expressed early in brainstem and skull development might result in abnormal or absent development of the abducens nerves, abnormal or absent development of inner ear and vestibular structures in the petrous bone, and/or other developmental anomalies affecting cerebral vasculature, the cardiovascular system, and orthopedic structures.³⁹ It seems conceivable that the FHF family of genes, represented here by the association of *FGF13* deletion with WS, may on occasion result in a similar phenotype in humans. Only additional studies in comparable patients will clarify this hypothesis.

DECLARATION OF INTEREST

The authors report no conflicts of interest. The authors alone are responsible for the content and writing of the paper.

This project was supported in part by the King Abdulaziz City for Science and Technology, Riyadh, Saudi Arabia [Project AT-30-20].

REFERENCES

1. Wildervanck LS. The cervico-oculo-acoustic syndrome. In: Vinken PJ, Bruyn GW, Myrathopoulos NC, editors. Handbook of Clinical Neurology. Amsterdam: North Holland, 1978; 32:123–130.
2. Kumar A, Sahu A, Shetty S, Vijayalakshmi P. Wildervanck syndrome associated with cleft palate and short stature. *Ind J Ophthalmol* 2010;58:323–325.

3. Cremers CW, Hoogland GA, Kuypers W. Hearing loss in the cervico-oculo-acoustic (Wildervanck) syndrome. *Arch Otolaryngol* 1984;110:54–57.
4. Balci S, Oguz KK, Firat MM, Boduroglu K. Cervical diastematomyelia in cervico-oculo-acoustic (Wildervanck) syndrome: MRI findings. *Clin Dysmorphol* 2002;11:125–128.
5. Brodsky MC, Fray KJ. Brainstem hypoplasia in the Wildervanck (cervico-oculo-acoustic) syndrome. *Arch Ophthalmol* 1998;116:383–385.
6. Strisciuglio P, Raia V, Di Meo A, et al. Wildervanck's syndrome with bilateral subluxation of lens and facial paralysis. *J Med Genet* 1983;20:72–73.
7. Hacıyakupoglu G, Pelit AA, Altunbasak S, et al. Crocodile tears and Dandy-Walker syndrome in cervico-oculo-acoustic syndrome. *J Pediatr Ophthalmol Strabismus* 1999;36:301–303.
8. Oe K, Mori K, Konno T, et al. Ruptured aneurysm of the sinus of Valsalva with Wildervanck syndrome (cervico-oculo-acoustic syndrome), blepharoptosis and short stature: case report. *Circulation J: Official J Japan Circ Soc* 2007;71:1485–1487.
9. Kumar A, Chaudhary D, Gupta SK. Wildervanck syndrome. *Aus Radiol* 1996;40:160–161.
10. Wettke-Schafer R, Kantner G. X-linked dominant inherited diseases with lethality in hemizygous males. *Hum Genet* 1983;64:1–23.
11. Tischfield MA, Bosley TM, Salih MA, et al. Homozygous HOXA1 mutations disrupt human brainstem, inner ear, cardiovascular and cognitive development. *Nat Genet* 2005;37:1035–1037.
12. Al-Baradie R, Yamada K, St Hilaire C, et al. Duane radial ray syndrome (Okiihiro syndrome) maps to 20q13 and results from mutations in SALL4, a new member of the SAL family. *Am J Human Genet* 2002;71:1195–1199.
13. Chan WM, Miyake N, Zhu-Tam L, et al. Two novel CHN1 mutations in 2 families with Duane retraction syndrome. *Arch Ophthalmol* 2011;129:649–652.
14. Traboulsi EI, Engle EC. Mutations in KIF21A are responsible for CFEOM1 worldwide. *Ophthalmic Genet* 2004;25:237–239.
15. Abu-Amero KK, Azad TA, Spaeth GL, et al. Unaltered myocilin expression in the blood of primary open angle glaucoma patients. *Mol Vis* 2012;18:1004–1009.
16. Clarke RA, Catalan G, Diwan AD, Kearsley JH. Heterogeneity in Klippel-Feil syndrome: a new classification. *Pediatric Radiol* 1998;28:967–74.
17. Smallwood PM, Munoz-Sanjuan I, Tong P, et al. Fibroblast growth factor (FGF) homologous factors: new members of the FGF family implicated in nervous system development. *Proc Nat Acad Sci USA* 1996;93:9850–9857.
18. Di Maio L, Marcelli V, Vitale C, et al. Cervico-oculo-acoustic syndrome in a male with consanguineous parents. *Can J Neurolog Sci* 2006;33:237–239.
19. Johnson NA, McClure MJ, Protzko E, Fosmire D. Wildervanck's syndrome presenting as hemiparesthesia. *Military Med* 1995;160:208–211.
20. Gupte G, Mahajan P, Shreenivas VK, et al. Wildervanck syndrome (cervico-oculo-acoustic syndrome). *J Postgrad Med* 1992;38:180–182.
21. Bosley TM, Alorainy IA, Salih MA, et al. The clinical spectrum of homozygous HOXA1 mutations. *Am J Med Genet A* 2008;146:1235–1240.
22. Bosley TM, Salih MA, Alorainy IA, et al. Clinical characterization of the HOXA1 syndrome BSAS variant. *Neurology* 2007;69:1245–1253.
23. Goldfarb M. Fibroblast growth factor homologous factors: evolution, structure, and function. *Cytokine Growth Factor Rev* 2005;16:215–220.
24. Goldfarb M, Schoorlemmer J, Williams A, et al. Fibroblast growth factor homologous factors control neuronal excitability through modulation of voltage-gated sodium channels. *Neuron* 2007;55:449–463.
25. Wu QF, Yang L, Li S, et al. Fibroblast growth factor 13 is a microtubule-stabilizing protein regulating neuronal polarization and migration. *Cell* 2012;149:1549–1564.
26. Guillemot F, Zimmer C. From cradle to grave: the multiple roles of fibroblast growth factors in neural development. *Neuron* 2011;71:574–588.
27. Geçz J, Baker E, Donnelly A, et al. Fibroblast growth factor homologous factor 2 (FHF2): gene structure, expression and mapping to the Borjeson-Forsman-Lehmann syndrome region in Xq26 delineated by a duplication breakpoint in a BFLS-like patient. *Human Genet* 1999;104:56–63.
28. Gartler SM, Goldman MA. Biology of the X chromosome. *Curr Opin Pediatr* 2001;13:340–345.
29. Franco B, Ballabio A. X-inactivation and human disease: X-linked dominant male-lethal disorders. *Curr Opin Genet Dev* 2006;16:254–259.
30. Morleo M, Franco B. Dosage compensation of the mammalian X chromosome influences the phenotypic variability of X-linked dominant male-lethal disorders. *J Med Genet* 2008;45:401–408.
31. Lowry RB, Jabs EW, Graham GE, et al. Syndrome of coronal craniosynostosis, Klippel-Feil anomaly, and sprenge shoulder with and without Pro250Arg mutation in the FGFR3 gene. *Am J Med Genet* 2001;104:112–119.
32. Miller MT, Stromland KK. What can we learn from the thalidomide experience: an ophthalmologic perspective. *Curr Opin Ophthalmol* 2011;22:356–364.
33. Barald KF, Kelley MW. From placode to polarization: new tunes in inner ear development. *Development* 2004;131:4119–4130.
34. Bok J, Bronner-Fraser M, Wu DK. Role of the hindbrain in dorsoventral but not anteroposterior axial specification of the inner ear. *Development* 2005;132:2115–2124.
35. Chisaka O, Musci TS, Capecchi MR. Developmental defects of the ear, cranial nerves and hindbrain resulting from targeted disruption of the mouse homeobox gene Hox-1.6. *Nature* 1992;355:516–520.
36. Abu-Amero KK, Kondkar AA, Salih MA, et al. Partial chromosome 7 duplication with a phenotype mimicking the HOXA1 spectrum disorder. *Ophthalmic Genet* 2012; (In Press).
37. Kohlhase J, Chitayat D, Kotzot D, et al. SALL4 mutations in Okiihiro syndrome (Duane-radial ray syndrome), acrorenal-ocular syndrome, and related disorders. *Hum Mutat* 2005;26:176–183.
38. Kohlhase J, Heinrich M, Schubert L, et al. Okiihiro syndrome is caused by SALL4 mutations. *Human Mol Genet* 2002;11:2979–2987.
39. Schneider-Maunoury S, Gilardi-Hebenstreit P, Charnay P. How to build a vertebrate hindbrain. Lessons from genetics. *Comptes Rendus de l'Academie des Sciences Serie III, Sciences de la Vie* 1998;321:819–834.